Computers and Electronics in Agriculture 66 (2009) 121–125

Contents lists available at ScienceDirect

Computers and Electronics in Agriculture

journal homepage: www.elsevier.com/locate/compag

Image pattern classification for the identification of disease causing agents in plants

A. Camargo[a,*], J.S. Smith[b]

[a] University of East Anglia, School of Computing Sciences, Norwich NR4 7TJ, UK
[b] Department of Electrical Engineering and Electronics, The University of Liverpool, Brownlow Hill, Liverpool L69 3GJ, UK

ARTICLE INFO

Article history:
Received 15 December 2005
Received in revised form 5 December 2008
Accepted 4 January 2009

Keywords:
Data classification techniques
Pattern recognition
Support Vector Machine
Image analysis

ABSTRACT

This study reports a machine vision system for the identification of the visual symptoms of plant diseases, from coloured images. Diseased regions shown in digital pictures of cotton crops were enhanced, segmented, and a set of features were extracted from each of them. Features were then used as inputs to a Support Vector Machine (SVM) classifier and tests were performed to identify the best classification model. We hypothesised that given the characteristics of the images, there should be a subset of features more informative of the image domain. To test this hypothesis, several classification models were assessed via cross-validation. The results of this study suggested that: texture-related features might be used as discriminators when the target images do not follow a well defined colour or shape domain pattern; and that machine vision systems might lead to the successful discrimination of targets when fed with appropriate information.

1. Introduction

The dramatic and worldwide spread of plant diseases is the driving force in the development of machine vision systems to identify these diseases. There is a need for systems that can help crop producers and farmers, particularly in remote areas, to identify early symptoms of plant disease by means of analyses of digital images of crop samples. The current electronic devices for capturing images have been developed to a point where there is little or no difference between the target and its digital counterpart. The success of machine learning for image pattern recognition also suggests applications in the area of identification of plant diseases.

Once the image of a target is captured digitally, a myriad of image processing algorithms can be used to extract features from it. The usefulness of each of these features will depend on the particular patterns to be highlighted in the image. Patterns are particular features of an image. They should be invariant to translation, rotation, and scale (Lee et al., 1999; Petersen et al., 2002; Shatadal and Tan, 2003; Ogiela and Tadeusiewicz, 2003), if potential misjudgements are to be avoided. The advantage of image classification by feature assessment is that patterns remain identical if preliminary conditions are changed. For example, pictures might be captured in conditions of different light intensity, or with different distances between camera lens and target. A key point in the implementation of optimal classifiers is the selection of features that characterise the image. Since there are many features to choose from, the job of selecting the best of them becomes cumbersome. A common practice to solve the problem of multiple features is to start out with as many of them as possible and implement a filter to discard those which add little or no information to the system (McNitt-Gray et al., 1995). Another approach is to use a small number of features that are known to be more representative of the target, and to rely on the classifier (Guo et al., 2001; Tang et al., 2000; Sena et al., 2003; King et al., 2000). In short, the success of any pattern recognition system will depend not only on the classifier, but also on the quality of the information the system is to differ from.

In this study we used image processing and pattern classification to implement a machine vision system that identified and classified the visual symptoms of plant diseases. For this purpose, multiple image based features were extracted from test images. A classifier assessed each of them individually and in groups. A set of candidate features was then selected. In turn, candidate features were used to identify the best classification model; we used Support Vector Machine as a machine learning method. The results of this study demonstrated that this method could be used to automatically identify symptoms of plant diseases.

2. Materials and methods

This study implements a machine vision system for the classification of the visual symptoms of plant diseases, from the analysis of coloured images. Diseased regions such as spots, stains or strikes

* *Corresponding author.* Tel.: +44 1603 456161; fax: +44 1603 458553.
E-mail address: a.camargo-rodriguez@uea.ac.uk (A. Camargo).

0168-1699/$ – see front matter © 2009 Elsevier B.V. All rights reserved.
doi:10.1016/j.compag.2009.01.003

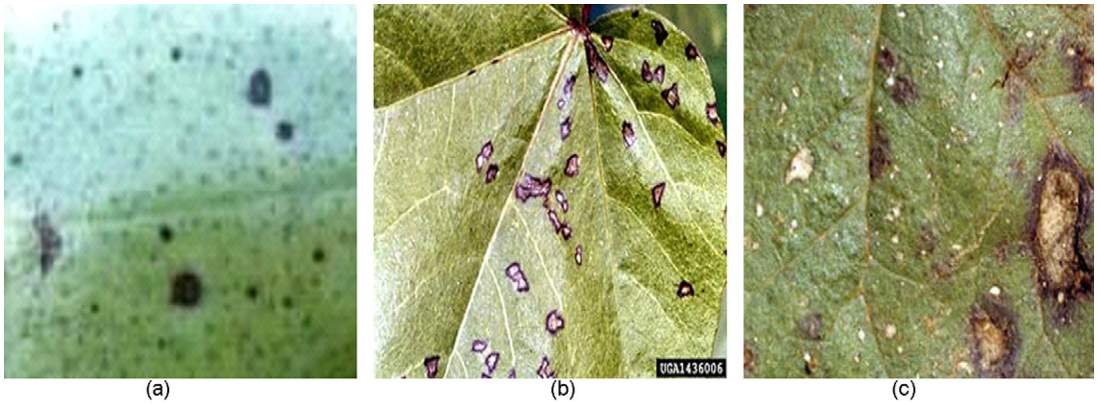

Fig. 1. Image of cotton crops showing the visual symptoms of damages caused by: (a) Southern green stink bug (*Nezara viridula*); (b) Bacterial angular (*Xanthomonas campestris*); (c) Ascochyta blight (*Ascochyta gossypii*).

were identified, segmented, pre-processed, and a set of image features was extracted from each region. Feature selection was then performed to identify which of these provided most information about the image domain. Those features that added little or no information were discarded. An SVM was used as a learning machine and cross-validation was the discrimination method used to identify the best classification model.

2.1. Image set

The set of 117 images of cotton crops used in this study was obtained from The Department of Entomology, at the University of Georgia, USA. Each image showed diseased regions, in different sections of the plant, i.e. leaf, fruit and stem, of a specific disease. In total, 26 images showed the damage caused by the green stink bug (Fig. 1a), 60 showed the damage caused by the Bacteria angular (Fig. 1b), and 31 showed the damage caused by the Ascochyta blight virus (Fig. 1c). In all cases, the image format used was JPEG, 24 bits.

2.2. Feature extraction

Target regions were identified and extracted using the method reported in our previous paper (Camargo and Smith, 2009). Target regions were those areas in the image that represented visual symptoms of a disease. Features that characterise the shape and appearance of an image, such as grey levels, connectivity and texture of an image were then extracted from each segmented region. Features corresponding to the last three categories were calculated from the image's RGB and HSV colour channels (Table 1).

2.3. Co-occurrence matrix

The co-occurrence matrix, among other existent techniques, was used to calculate image texture. This method measures occurrence of grey levels between a specific position $P(i, j)$ in the image and a neighbouring pixel, according to a given distance d and direction θ. Measurements that are possible to estimate via the co-occurrence matrix are: energy (Eq. (1.1)), inertia (Eq. (1.2)), entropy (Eq. (1.3)), homogeneity (Eq. (1.4)), and correlation (Eq. (1.5)). Each of these measurements were extracted from the image's RGB and HSV channels, when relative locations between pixels were at 0°, 45°, 90°, 135°, and within 1, 3 and 5 pixel-to-pixel distances. Finally, relative location measurements according to pixel distance were averaged, which resulted in one value for each distance (Pican et al., 1998).

$$\sum_i \sum_j p_d^2(i,j) \tag{1.1}$$

$$\sum_i \sum_j (i,j)^2 p_d(i,j) \tag{1.2}$$

$$-\sum_i \sum_j p_d(i,j) \log p_d(i,j) \tag{1.3}$$

$$\frac{\sum_i \sum_j p_d(i,j)}{1+(i-j)^2} \tag{1.4}$$

Table 1
Candidate features discriminated by categories.

Categories	Features	Description	Number of measurements
1	Shape	Solidity Extent Major axis length Minor axis length Eccentricity Centroid Diameter Area	8
2	Texture	d = 1, 3, 5	90
3	Fractal dimension	Box's size = 2, 4, 6, 8	4
4	Lacunarity	Box' size = 2, 4, 6, 8	4
5	Dispersion	RGB	3
6	Grey levels	For RGB and HSV channels	6
7	Grey histogram discrimination	For RGB and HSV channels	6
7	Fourier descriptor		20

$$\frac{\sum_i \sum_j p_d^2(i,j) - \mu_x \mu_y}{\sigma_x \sigma_y} \tag{1.5}$$

2.4. Fractal dimension

The fractal dimension feature measures the dimensions of an object. There are different techniques to estimate this measurement, one of them is known as the box-counting algorithm (Eq. (2)) (Falcone, 1990). Its functionality is based on placing a grid of pixels of length r over the image (I) and counting the number of boxes N covering it.

Given that r = box size; s = set; n = topological dimension of the set.

For any $r > 0$, let $N_r(I)$ be the minimum number of n-dimensional cubes of side-length r needed to cover I. If there is a number d so that:

$$N_r(I) \sim \frac{1}{r^d}; \quad r \to 0$$

Then the box-counting algorithm is defined as

$$\lim_{r\to 0} \frac{N_r(s)}{1/r^d} = k;$$

$$\lim_{r\to 0} (\ln N_r(I) + d \ln r) = \ln k,$$

solving for d gives

$$d = \lim_{r\to 0} \frac{\ln k - \ln N_r(I)}{\ln r} = -\lim_{r\to 0} \frac{\ln N_r(I)}{\ln r}, \tag{2}$$

where $\ln k$ is a constant

2.5. Lacunarity

This multi-scaled method measures the texture associated with patterns of spatial dispersion. The methodology used to calculate lacunarity was the Gliding Box Algorithm (Plotnick et al., 1993). a $r \times r$ box (minimum r = 2) is placed over the upper left corner of an image. The number of occupied sites (S) is referred to as the box mass. The box is moved one column to the right and the box's mass is again measured. This process is repeated over all rows and columns which produces the frequency distribution of the box's mass. The number of boxes r containing S occupied sites is given by $n(S, r)$ and the total number of boxes of size r is given by $n(r)$. The probability of distribution is given by:

$$Q(S,r) = \frac{n(S,r)}{N(r)}$$

The first and second moments of this distribution is determined by

$$z^{(1)} = \sum SQ(S,r)$$
$$z^{(2)} = \sum S^2 Q(S,r)$$

The first and second moments can also be described by the mean $E(S)$ and variance $Var(S)$ of the box masses as:

$$z^{(1)} = E(S)$$
$$z^{(2)} = Var(S) + E^2(S)$$

As a result, the lacunarity index (Λ) for a box of size r is defined as (Eq. (3)):

$$\Lambda(r) = 1 + \left(\frac{Var(S)}{E^2(S)}\right) \tag{3}$$

2.6. Evaluation of diagnostic models

A machine learning method based on a SVM was used to identify the best classification model. SVMs for pattern recognition problems have become popular due to its effectiveness in real classification problems (Cherian et al., 2004; Foody and Mathur, 2004; Hearst, 1998). We hypothesised that given the characteristics of the images, there should be a subset of features more informative of the image domain. To test this hypothesis, several classification models were assessed by cross-validation. The number and type of image features varied amongst models. To overcome the problems of nonlinearity and multiple classes classification, the SVM classifier used the Radial Basis Function (RBF) kernel and the one-against-one method respectively. The set of features extracted from the 117 image samples were labelled according to the disease they belonged to, i.e. one (1) for the stink bug, two (2) for the Bacteria angular, and three (3) for the Ascochyta blight virus.

2.7. SVM classifier

In a SVM a linear training sample is separable by a hyperplane according to the decision function $f(x) = \text{sign}(w \cdot x) + b$, where w is a weight vector and b is a threshold cut-off. To maximise the margin $w \in f$ and b have to be minimised to:

$$y_i(w \cdot x_i) + b \geq 1,$$

which can be formulated as a quadratic optimisation problem

$$\min_{w,b} \frac{1}{2} ||w||^2$$

Additional slack variables should be added to nonlinearly separable cases with a risk of overfitting.

$$y_i(w \cdot x_i) + b \geq 1 - \xi_i,$$

therefore the SVM requires the solution of this optimisation problem (Eq. (4)):

$$\min_{w,b,\xi} \frac{1}{2} ||w||^2 w + C \sum_{i=1}^{l} \xi_i, \tag{4}$$

where C is a constant of regularisation that determines the trade-off between training error and the complexity term (confidence).

A SVM maps the training vectors into a higher dimensional space f via a nonlinear map Φ: $R^n \to f$, then $\Phi(x_i)$ is substituted for each training sample x_i and the conditions for perfect classification are

$$y_i((w \cdot \Phi(x_i)) + b) \geq 1 - \xi_i,$$

Given a training set of instance-label pairs (x_i, y_i), $i = 1 \ldots l$, where $x_i \in R^n$ and $y \in \{1, -1\}^l$, the support vector machines (SVM) (4) require the solution of the following optimisation problem (Hsu et al., 2004):

2.8. Multiple classes classification

When the problem of classification involves more than two classes, as it is the case in this study, a number of methods can be used to deal with this very common scenario. We used the one-against-one (Hsu and Lin, 2002; Angulo et al., 2003) method, which constructs $k(k-1)/s$ classifiers where each one is trained on data from two classes. For training data from the jth classes, the following

Table 2
Results of testing analysis on candidate features. (a) Every feature tested individually (Individual %). (b) Groups were used as inputs (Group %). (c) Whole set of candidate features (53) were used as inputs to the classifier (All set). (d). Features whose retrieval caused an improvement in classification accuracy. (e) All except retrieved features were used as inputs to the classifier.

Tag	Group	Feature	Individual %	Group %	All set %	Retrieved	All—LOO
1	Shape	Solidity	52.4	55.0	90.0		93.1
2		Extent	57.13				
3		Minor axis length	57.26			x	
4		Eccentricity	50.42			x	
5	Texture	Texture R′1	53.0	83.0			
6		Texture R′2	52.13				
7		Texture R′3	53.0				
8		Texture R′4	55.0				
9		Texture R′5	52.13				
10		Texture G′1	52.13				
11		Texture G′2	52.13				
12		Texture G′3	53.0				
13		Texture G′4	55.0				
14		Texture G′5	52.13				
15		Texture B′1	52.13				
16		Texture B′2	52.13				
17		Texture B′3	52.13				
18		Texture B′4	56.0				
19		Texture B′5	52.13				
20		Texture H′1	59.0				
21		Texture H′2	61.0				
22		Texture H′3	60.1				
23		Texture H′4	61.0				
24		Texture H′5	59.0				
25		Texture S′1	53.0				
26		Texture S′2	54.0				
27		Texture S′3	54.0				
28		Texture S′4	54.0				
29		Texture S′5	54.0				
30		Texture V′1	50.1				
31		Texture V′2	50.1				
32		Texture V′3	55.0			x	
33		Texture V′4	50.1				
34		Texture V′5	50.1				
35	Fractal dimension	Fractal dimension	50.1	50.0		x	
36	Lacunarity	Lacunarity 2	50.1	52.13		x	
37		Lacunarity 4	50.1			x	
38	Dispersion	Dispersion R	62.0	73.0			
39		Dispersion G	57.2				
40		Dispersion B	52.1				
41	Grey level	Grey R	56.0	68.0			
42		Grey G	56.0				
43		Grey B	60.0				
44		Grey H	60.1				
45		Grey S	53.0				
46		Grey V	53.0				
47	Histogram of frequencies	Gray_hist R	63.0	68.3			
48		Gray_hist G	56.0			x	
49		Gray_hist B	50.4				
50		Gray_hist H	62.0			x	
51		Gray_hist S	51.2				
52		Gray_hist V	50.0				

binary classification has to be solved (Eq. (5)):

$$\min_{w,b,\xi} \frac{1}{2}(w^{ij})^T w^{ij} + C\sum_t \xi_t^{ij}(w^{ij})^T \tag{5}$$

$$(w^{ij})^T \phi(x_t) + b^{ij} \geq 1 - \xi_t^{ij} \quad \text{if}_y t = i$$
$$(w^{ij})^T \phi(x_t) + b^{ij} \leq -1 + \xi_t^{ij} \quad \text{if}_y t = j \quad \xi_t^{ij} \geq 0$$

A SVM is a parameterised function whose functional form is defined according to the type of data to be manipulated. Therefore, cross-validation was applied to select optimal RBF's parameters ($C = 100$, $\alpha = 0.01$), and to test classifier models for each testing scheme involved in the study.

2.9. Feature selection

For the identification of the best classification model three approaches were used. (1) Each feature was used as single input to the classifier. (2) Groups of features were used as inputs to the classifier. (3) All features except one were used as the input set. In all cases, seven-fold cross-validation was used as the evaluation method. In other words, the data set was divided into seven subsets, one of this was used as the testing set and the other remaining subsets were used as the training set. This process was repeated until each subset has been used as the testing set. Finally, the average error across all trials was computed.

3. Results

Results of testing showed that the following features could not be a part of the image classifier.

(1) Area, Perimeter, Centroid and Diameter. When any of these four was used as individual input to the classifier, average classification accuracy was below 50%.
(2) FDs. They failed to retrieve significant measurements from relatively small images (∼<300 pixels). To solve this limitation, small images were resized via the bicubic interpolation and the amount of descriptors was reduced to 20. Unfortunately, the new estimation of FDs showed no significant changes to the measurements initially obtained.
(3) Texture when the distance between pixels was either one or three. When either of these features was used as a single input to the classifier, average classification accuracy was below 50%.
(4) Lacunarity, where the box's dimension was either six or eight pixels. Either of these features used as single inputs to the classifier conveyed average classification accuracy below 50%. The remaining features (53), shown in Table 2, resulted in an average classification accuracy of above 50% when used as single inputs to the classifier.

Once candidate features were identified, groups of them, according to their domain (e.g. Shape, Texture, Dispersion, etc.), were used as inputs to the classifier. With this procedure we found that features composing the group texture achieved the highest classification rate (83%) and features composing the group shape achieved the lowest (55%). On the contrary, when all features (53) were used as inputs, classification accuracy was 90% (Table 2). This method did not provide enough evidence to withdraw groups of features, rather it suggested the use of the whole set.

The last testing procedure looked at how much the accuracy rate, set in 90% for all features, decreased or increased when one feature was withdrawn at a time. If the rate increased when the feature was withdrawn, the feature was discarded. If the rate decreased, the feature was kept. The procedure finished when all possibilities were exhausted. The use of this testing procedure identified the best classification model which was achieved with 45 features and whose classification accuracy was set to at 93.1%. Discarded features are shown in Table 2 under the column retrieved. They are highlighted with the symbol 'x'.

4. Conclusions

The identification of the symptoms of plant diseases by means of a machine vision system may support farmers during their daily struggle against disease outbreaks. Here we used digital images of crop plants that showed visual symptoms of a particular disease. These diseased regions were identified and segmented with the help of an algorithm as previously reported. Features were extracted from each segmented region and used as inputs to a classifier. Because not all features were supposed to give the same amount of information about the target, we used cross-validation to identify those which comprised the best classification model. The results of this study were primarily two-fold. Firstly, the measurements of texture can be used as a useful discriminator for these types of images. Secondly, machine learning systems can be used to identify the visual symptoms of plant diseases and this may have a particular application for farmer or crop produces in remote locations.

Acknowledgement

We thank Dr. Chih-Jen Lin for providing the LibSVM software and also for clarifying some doubts about SVM.

References

Angulo, C., Parra, X., Catala, A., 2003. K-SVRC. A Support Vector Machine for multiclass classification. Neurocomputing 55, 57–77.
Camargo, A., Smith, J., 2009. An image processing-based algorithm to automatically identify plant disease visual symptoms. Biosystems Engineering 102 (1), 9–21.
Cherian, G., Song, X., Fan, G., Rao, M.N., 2004. Application of Support Vector Machines for Automatic Compliance Monitoring of the Conservation Reserve Program (CRP) Tracts. In: Proc. IEEE International Geosciences and Remote Sensing Symposium (IGARSS2004), pp. 20–24.
Falcone, K.r., 1990. Fractal Geometry—Mathematical Foundations and Applications. John Wiley & Sons, Chichester.
Foody, G.M., Mathur, A., 2004. A relative evaluation of multiclass image classification by support vector machines. IEEE Transaction Geosciences and Remote Sensing 99, 1–9.
Guo, G., Li, S.Z., Chan, K.L., 2001. Support vector machines for face recognition. Image and Vision Computing 19, 631–638.
Hearst, M.A., 1998. Support Vector Machines. IEEE Intelligent Systems 13 (4), 18–28.
Hsu, C.W., Lin, C.J., 2002. A comparison of methods for Multi-class Support Vector Machines. IEEE Transaction on neural networks 13 (2), 415–425.
Hsu, C.W., Chang, C.C., Lin, C.J. A practical guide to support vector classification. (Online). Available: http://www.csie.ntu.edu.tw/∼cjlin/papers/guide/guide.pdf. Accessed: 8 March 2004.
King, S.L., Bennett, K.P., List, S., 2000. Modelling noncatastrophic individual tree mortality using logistic regression, neural networks, and support vector methods. Computers and Electronics in Agriculture 27 (1–3), 401–406.
Lee, J.W., Lee, H.W., Lee, J.H., Kang, I.T., Lee, G.K., 1999. A study on Lung Nodule detection using neural networks. IEEE Tencon, 1150–1153.
McNitt-Gray, M., Huang, H.K., Sayre, W.J., 1995. Feature selection in the pattern classification problem of Digital Chest Radiograph segmentation. IEEE Transaction Medical Imaging 14 (3), 537–547.
Ogiela, M.R., Tadeusiewicz, R., 2003. Artificial intelligence structural imaging techniques in visual pattern analysis and medical data understanding. Pattern Recognition 36 (10), 2441–2452.
Petersen, M.W., Ridder, D., Handels, H., 2002. Image processing with neural networks—a review. Pattern recognition 35, 2279–2301.
Pican, N., Trucco, E., Ross, M., Lane, D.M., Petillot, Y., Tena, I.R., 1998. Texture analysis for seabed classification: co-ocurrence matrices vs self-organization maps. In: Proceedings from Oceans' 98, Nice, pp. 424–428.
Plotnick, R.E., Gardner, R.H., O'Neill, R.V., 1993. Lacunarity indices as measures of landscape texture. Landscape ecology 8 (3), 201–211.
Sena, D.G., Pinto, F.A.C., Queiroz, D.M., Viana, P.A., 2003. Fall armyworm damaged maize plant identification using digital images. Biosystems Engineering 85 (4), 449–454.
Shatadal, P., Tan, J., 2003. Identifycation damaged soybeans by colour image analyses. Applied engineering in agriculture 19 (1), 65–69.
Tang, Y.Y., Tao, Y., Lam, E.C.M., 2000. New method for feature extraction based on fractal behaviour. Pattern recognition 35, 1071–1081.